

Research Article

Chinnasamy Rajendran*, Kasi Srinivasan, Visvalingam Balasubramanian, Haridasu Balaji, and Ponnumuthu Selvaraj

Mechanical properties and microstructural characteristics of friction stir welded AA2014-T6 aluminium alloy joints

<https://doi.org/10.1515/jmbm-2019-0019>

Received Mar 01, 2019; accepted Dec 10, 2019

Abstract: The quality of friction stir welded joints depends upon the working parameters such as rotational speed, welding speed, shoulder diameter, tilt angle; etc. Each process parameter has a significant effect on the formation of joint strength. This investigation attempts to understand the effect of friction stir welding parameters on microstructural characteristics and tensile strength of AA2014-T6 aluminium alloy. This is performed by changing any one of the process parameters from minimum to maximum and keeping others constant. The joint fabricated from a rotational speed of 1500 rpm, welding speed of 40 mm/min, shoulder diameter of 6 mm and tilt angle of 1.5° yielded superior tensile properties compared to their counter joints. Due to the formation of defect-free weld, balanced material flow and uniform distribution of strengthening precipitates in the stir zone is achieved.

Keywords: 2014 Al-Cu alloy, Friction stir welding, Process parameters, Microstructure, Tensile properties

1 Introduction

Aluminium alloy (2xxx) has a high strength to weight ratio, good formability and high corrosion resistance and it has been widely used as a critical structural material in many industries, such as aerospace, shipbuilding and automobile. Nevertheless, Al alloy is very difficult to weld by

fusion welding process. It causes hot cracking, alloy segregation, partially melted zone and porosity. Hence, careful consideration is required to weld high strength Al alloys using fusion welding process. Experimental results prove that that fusion welding was not suited for joining of high strength Al alloy [1]. Friction stir welding (FSW) as an innovative solid-state process has proved effectively and efficiently to weld lightweight metals, such as Al and Mg alloys [2, 3]. FSW completely eliminates fusion welding problems and acts as a replacement for mechanical fasteners like screw, bolt & nut and rivets. However, FSW has resulted in softening of the joints and degradation of mechanical properties [2, 4], which is particularly in the FSW joints of precipitation hardening Al alloys (e.g., 2xxx [5, 6] and 7xxx series Al alloys [7, 8]) and dissimilar joints of Al and Mg alloys [9–11], because of the dissolution and growth of strengthening precipitates. Therefore, a better quality of friction stir weld can be achieved by controlling the FSW parameters. Zhang *et al.* [12] studied the effect of welding parameters on microstructure and mechanical properties of FSW joints of super high strength Al-Zn-Mg-Cu alloy. The result showed that the grain size in the stir zone (SZ) decreases by increasing welding speed or decreasing rotational speed during FSW, subsequently it is understood that the strengthening precipitates in the heat-affected zone (HAZ) were deteriorated and coarsened due to thermal cycle.

Muthu *et al.* [13] analyzed the effect of pin profile and process parameters on microstructure and mechanical properties of FSW Al-Cu joints, by incorporating three types of pin profile such as whorl, plain taper and taper threaded. Out of three pins, plain taper pin had a defect free SZ and high strength. Ma *et al.* [14] experimented to investigate the effect of process parameters and fatigue properties of FSW of AA2198-T6 aluminium - lithium alloy joints. The results show that the microhardness and strength of the joint through the weld decrease with increasing the tool rotational speed to welding speed ratio. Similarly, the fracture mode was changed from brittle

***Corresponding Author: Chinnasamy Rajendran:** Department of Mechanical Engineering, Sri Krishna College of Engineering and Technology, Coimbatore, India-641008; Email: crdm12@yahoo.com

Kasi Srinivasan, Visvalingam Balasubramanian: Centre for Materials Joining and Research, Department of Manufacturing Engineering, Annamalai University, Annamalainagar-608002

Haridasu Balaji, Ponnumuthu Selvaraj: Aeronautical Development Agency, Bangalore

Table 1: Chemical composition (wt. %) of base material

Si	Fe	Cu	Mn	Mg	Zn	Cr	Ti	Al
0.87	0.13	4.81	0.81	0.73	0.06	0.005	0.01	Balance

Table 2: Mechanical properties of base material

Material	0.2% Yield stress (MPa)	Ultimate tensile stress (MPa)	Elongation in 50 mm gauge length (%)	Micro hardness 0.5 N, 15 sec (HV)
AA2014-T6	431	455	10	163

tle to ductile mode. Xu *et al.* [15] reported the influence of welding parameters and tool pin profile on microstructure and mechanical properties along with the thickness in a FSW aluminium alloy. They were reported to be the top showed large equiaxed grain structure and finer second phase strengthening precipitates compared with the rear and middle of the SZ. Ramachandran *et al.* [16] analyzed the effect of tool rotational speed on characteristics of dissimilar FSW aluminum alloy AA5052 and high strength low alloy steel joints. The FSW trails were conducted by varying the traverse speed and holding the other parameters constant. It was found that the maximum tensile strength of 91% to the strength of base Al alloy was achieved at a traverses speed of 45 mm/min. Sharma *et al.* [17] used Al-Zn-Mg alloy to investigate the effect of welding process parameters on microstructure and mechanical properties of FSW joints of 7039 Al alloy. They concluded that the mechanical properties of the welded joints, improved with increasing tool rotational speed or decreasing welding speed.

Singh *et al.* [18] analyzed that the effect of FSW parameters on microstructural characteristics and mechanical properties of 6082-T651 Al alloy joint. The welding speed and tool rotational speed were important parameters on the formation of quality welds and the maximum tensile strength obtained was 263 MPa, which was 85% of base metal. Cai *et al.* [19] investigated the effect of FSW parameters on the mechanical properties and microstructural characteristics of 2060 Al-Cu-Li alloy joints. The base material was composed of T1 precipitates with small quantities of θ' and S' . The various strengthening precipitates were dissolved in the SZ, where dense dislocation and nano-sized co-cluster were found. Furthermore, the effect of welding speed on microstructure and hardness in the FSW joints of 6005A-T1 aluminium alloy joints. The welding speed had no significant influence on the thermo-mechanically affected zone (TMAZ) region hardness, due to the elongated grains and density of dislocations. If, the heat-affected zone located near the weld centre line the

hardness was lower and higher for far from the weld centre line due to coherent of β' precipitates [20]. Liu *et al.* [21] investigated the effect of process parameters on FSW of dissimilar aluminium alloy with advanced high strength steel. The utmost strength could reach 85% of base aluminium alloy due to formation of an intermetallic layer of Fe-Al or Fe₃Al with a thickness of 1 μ m was presented at the Al-Fe interface region in the advancing side.

From the literature [12–21], it is understood that a lot of research work has been carried out to investigate the effect of individual friction stir welding parameter on microstructural characteristics and tensile properties of different grade of aluminium alloys. To the best knowledge of the authors, no studies are conducted to analyze the combined effect of rotational speed, welding speed, shoulder diameter and tool tilt angle on microstructural characteristics and tensile properties of friction stir welded joints of AA2014-T6 aluminium alloy.

2 Experimental work

The base material used in this investigation was AA2014-T6 aluminium alloy sheet of 2 mm thick with dimensions of 300 long and 150 mm wide, whose chemical composition and mechanical properties are listed in Table 1 and Table 2 respectively. Figure 1a shows the microstructure of base material. It consists of coarse and elongated grains which oriented along the rolling direction. The samples were longitudinally butt welded using computer numeric controlled friction stir welding machine (Figure 1b). Fabricate non-consumable tools consist of the plain concave shoulder with left hand threaded to taper cylindrical pin (Figure 1c). The fabricated welding tool dimensions and FSW parameters used in this study are presented in Table 3 and Table 4 respectively. After welding (Figure 1d), the joints were all sectioned perpendicular to the welding direction for metallography observation and tensile test

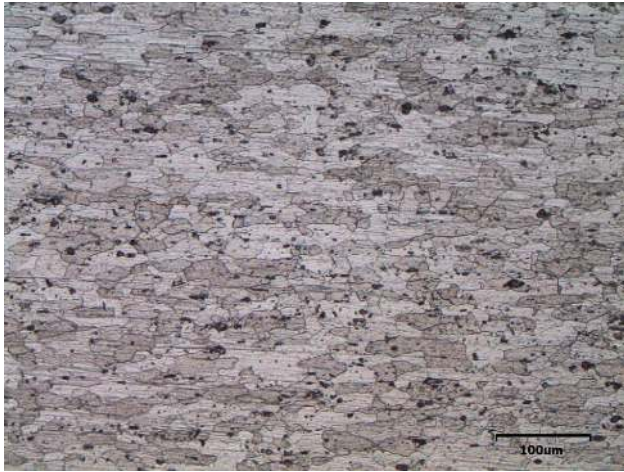


Figure 1: Micrograph of base metal

Table 3: FSW tool dimensions

Sl. No	Process parameters	Values
1	Pin type	Left hand threaded taper cylindrical pin
2	Major diameter of pin	2 mm
3	Minor diameter of pin	1.5 mm
4	Screw pitch	1.2 mm
5	Shoulder type	Concave
6	Shoulder concavity	1°

(Figure 1e,1f). Metallography observation was carried out by an optical microscope. The specimens were polished with alumina suspension etched by Keller's reagent for macro and microstructure. The sizes of the tensile specimens were prepared by the reference to the ASTM-E8-M04 and the marked gauge length and width of 50 mm and 12.5 mm respectively. A room temperature tensile test was carried out with a crosshead velocity of 1.5 mm/min. The microhardness measurement was carried out across the cross-section of the weld with a constant load of 50 N and dwell time of 15 s. Scanning electron microscopy (SEM) was used to analyze the fracture morphology of the joints. Energy-dispersive spectroscopy (EDS) was used to identify the percentage of an element presented in the weld region.

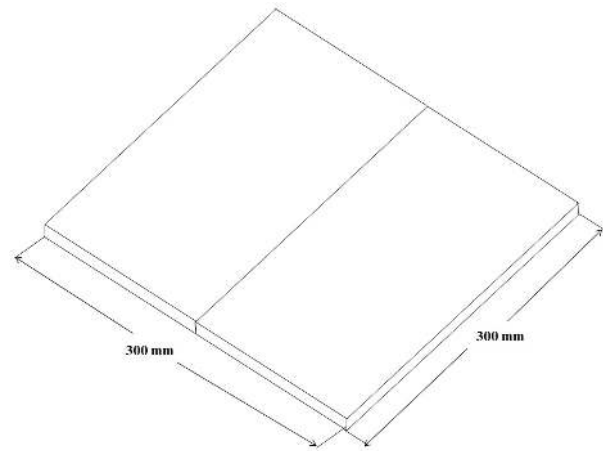


Figure 2: Schematic diagram of butt joint

3 Results

3.1 Surface morphology

Figure 2 Shows the surface morphology of the friction stir welded joints under different welding conditions using predominant process parameters such as rotational speed, welding speed, shoulder diameter and tilt angle. The joint fabricated using a rotational speed of 1500 rpm, welding speed of 50 mm/min, shoulder diameter of 6 mm and tilt angle of 1.5° exhibited higher tensile strength compared to other joints. Also, the surface appearance of all joints is smooth. Slight and severe delamination surface was found in the weld line when the joint welded at a rotational speed of 1100 rpm and 1900 rpm respectively. For both the rotational speed, the joint surface was rough at lower rotational speed and produced a lack of fill defect. Even though the joint surface was smooth at higher rotational speed, the warm hole defect was found under the surface of the weld due to higher heat input during FSW. Further, the testing of these two joints was not carried out. The joint fabricated with the various welding speed as shown in Figure 2, it could be noted that severe plastic deformation was found at a low welding speed of 10 mm/min due to severe heat input, as it results in warm hole defect. At higher welding speed of 70 mm/min, the surface was found to slight delamination and lack of filling defect, because, the contact time of the shoulder and surface of the sheet was low. However, heat input is inversely proportioned to the welding speed [22]. Hence, testing of these two joints was not carried out in the further investigation. At shoulder diameter of 2 mm and 10 mm appearance of less and severe plastic deformation was observed. For both the shoulder diameter, the joint surface was rough at low shoulder diam-

Table 4: Effect of FSW parameters on tensile strength

Joint No	Cond.	Parameters		Micro hardness 0.5 N 15 S	Elongation in 50 mm gauge length (%)	0.2% Yield strength “MPa”	Ultimate tensile strength “MPa”	Joint efficiency “%”
1	Effect of tool rotational speed “rpm”	1100		102	3.1	155	202	44
2		1300	40 mm/min	121	3.3	166	218	56
3		1500	6 mm	128	5.9	285	376	82
4		1700	1.5°	123	4.2	205	242	53
5		1900		108	2.9	165	212	46
6	Welding speed “mm/min”	10		101	3.2	174	208	46
7		20	1500 rpm	121	4.9	185	239	52
8		40	6 mm	130	5.8	279	381	83
9		60	1.5°	125	4.1	201	261	58
10		70		109	3.3	156	210	47
11	Shoulder diameter “mm”	2		108	2.8	186	255	56
12		4	1500 rpm	119	4.8	255	314	69
13		6	40 mm/min,	131	5.4	312	378	83
14		8	1.5°	128	4.6	296	361	79
15		10		111	3.0	196	232	51
16	Tool tilt angle “°”	0.0		108	2.8	155	198	44
17		0.5	1500 rpm	121	2.9	181	204	45
18		1.5	40 mm/min,	134	5.5	312	377	82
19		2.5	6 mm	125	4.1	201	247	54
20		3.0		114	3.2	191	212	47

eter, tunnel defect was visually obtained. At high shoulder diameter of 10 mm produced high heat input and causes warm hole defects in the weld. Hence, these two joints have not used for further study. Figure 2 shows the surface morphology of the friction stir welded joints under various tilt angles, it can be observed that the joint fabricated with 1.5° exhibited smooth surface compared with other joints. At low tilt angle of 0° (*i.e.*) tool positioned normal to the welding line, appearance of lack of fill and poor material consolidation observed. Due to insufficient material flow and insufficient forging force. At higher tilt angle of 3° showed severe plastic and excess flash, material come out between the bottom of the shoulder to the top surface of the sheet. Like its results, the effective sheet thickness was reduced. Hence, the characterization of these two joints was not involved in this investigation.

3.2 Mechanical properties

Table 4 and Figure 3a-3d represent the average tensile properties of friction stir welded alloy joints under different process parameters. It is evident from the Table 4 that

**Figure 3:** Photograph of fabricated tools

the yield strength, ultimate tensile strength and % elongation of friction stir welded joints are inferior to the base material. At constant welding speed of 40 mm/min, shoulder diameter of 6 mm and tilt angle of 1.5° with increas-



Figure 4: Photograph of fabricated joints

ing in rotational speed from 1300 rpm to 1500 rpm, the strength, yield strength and % elongation increased to 376 MPa, 285 MPa and 5.9% respectively. At constant rotational speed of 1500 rpm, shoulder diameter of 6 mm and tilt angle of 1.5, an increasing welding speed of 20 mm/min to 40 mm/min almost linearly increased to strength, yield strength, % elongation of 381 MPa, 279 MPa and 5.8 % respectively. Further, strength decreased with increasing the welding speed of 60 mm/min. From the Figure 3c, it can be understood that an increase in shoulder diameter from 4 mm to 6 mm (constant 1500 rpm, 40 mm/min, 1.5) linearly increased the strength, yield strength and % elongation from 314 MPa to 378 MPa, 255 MPa to 312 MPa and 4.8% to 5.4%, respectively. Further, decreased with increasing shoulder diameters to 8 mm. Similarly, the increase in tilt angle (constant 1500 rpm, 40 mm/min, 6 mm) from 0.5 to 1.5 increased strength, yield strength and % elongation to 377 MPa, 312 MPa and 5.5% respectively. From the tensile test result, it is understood that the joint fabricated at the rotational speed of 1500 rpm, welding speed of 40 mm/min, shoulder diameter of 6 mm and tilt angle of 1.5° yielded superior mechanical properties.

3.3 Microhardness

Many microhardness profiles should be placed in evidence against the effect of FSW parameters. Figures 4a-4d shows the microhardness distribution of transverse cross-section of the weld under different processing parameters. The joint exhibited typical W shaped hardness profile. The hardness of the FSW joints (average of 101 HV -134 HV)

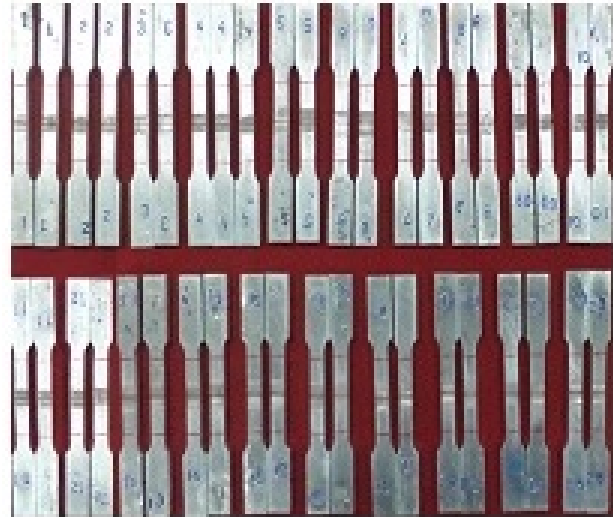


Figure 5: Photograph of tensile specimen (Before testing)

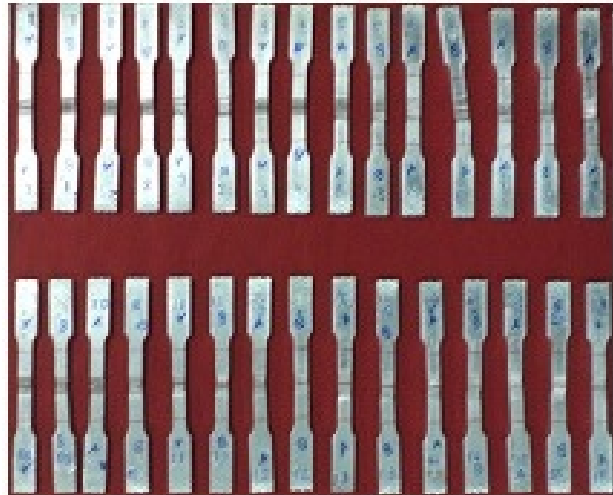


Figure 6: Photograph of tensile specimens (After testing)

was lower than the base material (155 HV). Hardness of SZ was higher than the TMAZ and can reach base material hardness level. It could indicate that the hardness of SZ was greater dependence on FSW parameters like rotational speed, welding speed, shoulder diameter and tilt angle. There are two primary reasons for improved SZ hardness, first one is formation of sub grains (fine grains) due to dynamic recrystallization and second one, the density distribution of precipitates during FSW. Each joint has two soft regions (low hardness region), one on the advancing side and the another on the retreating side. The location of soft region was obviously different from irrespective of process parameters. The average microhardness in the SZ increased from 102 HV to 128 HV with increasing the rota-

tional speed from 1300 rpm to 1500 rpm, while the average microhardness decreases from 128 HV to 123 HV with increasing rotational speed from 1500 rpm to 1700 rpm. Similarly, the average microhardness in the SZ increased from 121 HV to 130 HV, 126 HV to 131 HV and 126 HV to 134 HV, while increasing welding speed from 20 mm/min to 40 mm/min, shoulder diameter from 4 mm to 6 mm and tilt angle from 0.5 to 1.5 respectively. Hardness has been decreased to 125 HV, 128 HV and 125 HV, while increasing welding speed of 60 mm/min, shoulder diameter of 8 mm and tilt angle of 2.5° respectively. These results of microhardness are in good agreement to the tensile strength and grain size

3.4 Microstructure

As a result of the rolling process, the base material consists of coarse and elongated grains, which are oriented along the rolling direction with un-even distribution of strengthening precipitates. The average grain size of the base material was 30 μ m. Figures 5-8 showed the set of figures related to the optical micrograph under individual parameter effect on friction stir welded joints. Based on the material flow and grain sizes, the joints were classified into three regions such as SZ, TMAZ and the base metal. The SZ microstructure is characterized by recrystallized, fine and equiaxed grains. A complex flow structure consists of upward elongated grains, was observed in the TMAZ on both retreating side (Figures 5-8a-c) and advancing side (Figures 5-8e-i), on the other hand unaffected base material. All the SZ invariably contains fine and equiaxed grains (Figures 5-8d-f). Because of severe plastic deformation and high peak temperature to cause dynamic recrystallization, caused by rotation and transverse motion of tool during FSW. The large and elongated grains converted into fine and equiaxed grains in the SZ. As compared to the base material fewer second phase precipitates, of Al₂Cu were observed in the SZ as these were broken down and uniformly distributed by stirring of the tool. The image analysis of the weld microstructure was done using image analyzing software. To determine the average grain size of α -aluminum presented in the SZ. It is understood that increasing the rotational speed from 1200 to 1500 rpm decreases the grain size (7.09 μ m), further increasing the rotational speed to 1700 rpm the grain size (12.21 μ m) increases. Due to high rotational speed, it generates high heat input and reduced the cooling rate. As its results, grain coarsening was observed [23]. Hence, the grain size increased. Similarly, the increasing in welding speed decreases the average grain size of SZ (8.9 μ m), due to low level of heat

input and allows its faster cooling rate and prevents grain coarsening. While increasing the shoulder diameter to 6 mm, the average grain size in the SZ (7.81 μ m) decreased and increased from increasing shoulder diameter to 8 mm (9 μ m), because the area under the small size shoulder produced low heat input that causes less plastic flow of material, on the other hand larger diameter shoulder occupy larger area and heat input was more. The tool tilt angle is the important parameter for joining high strength aluminum alloys; it can eliminate lack of filling defect and improper forging force. From the Table 4, the increasing tilt angle to 1.5° decreased the grain size and increased with increasing to tilt angle to 3°. Because increasing the tilt angle increased forging forces in addition to high heat input and reduced the effective sheet thickness.

3.5 Fractograph

Tables 5-8 enlisted the effect of FSW parameters on fracture morphology of friction stir welded joints under different processing parameters. Fracture of defect free sound welded joints during a tensile test took place from fractured region. All the joints were fractured in the advancing side, and conforming, it is softer and weaker region than another region. It is believed that the locations of the lowest hardness across the welded joints are dependent on heat input and FSW parameters. The high heat input welded joints showed minimum hardness in the TMAZ region. While that in case of low heat input welded joint was found in the SZ. Variation in rotational speed at constant welding speed, shoulder diameter and tilt angle results in change of fracture location from SZ to TMAZ (1300 rpm to 1500 rpm). And joint fabricated from the rotational speed of 1700 rpm, the fracture location shifted to the weld center. At low welding speed of 20 mm/min, the joint, fractured at the SZ /TMAZ interface, while increasing the welding speed of 60 mm/min, the fracture location was observed at the SZ. Similarly, at larger shoulder diameter and high tilt angle produced high heat input and the fracture location was observed at the SZ/TMAZ interface. The joint fabricated from the small shoulder diameter (4 mm) and low tool tilt angle (0.5°) fractured at the SZ due to low heat input.

4 Discussion

During FSW, the quality of joint was closely related to the flow of material in and around the tool pin. Based on the

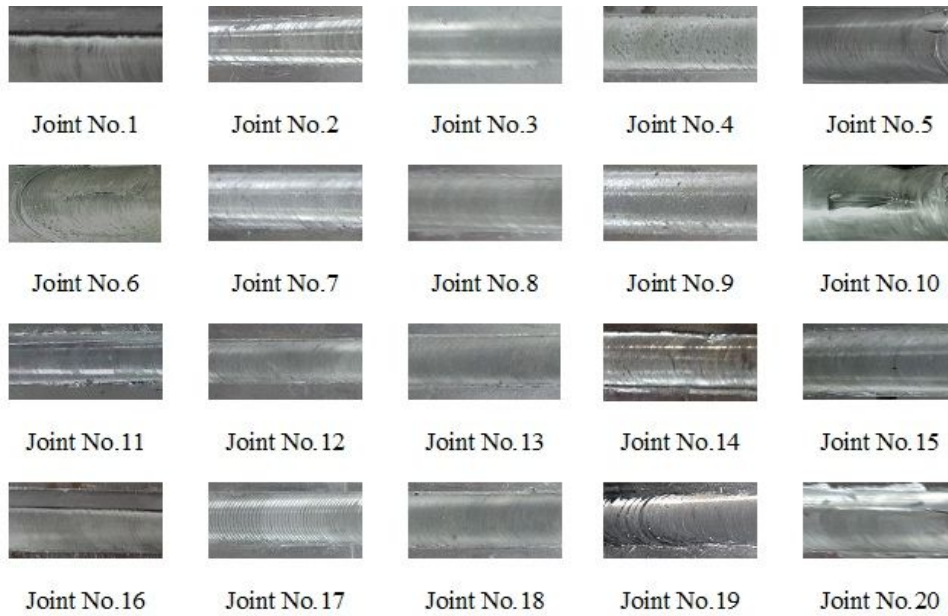


Figure 7: Effect of FSW parameters on macrostructure

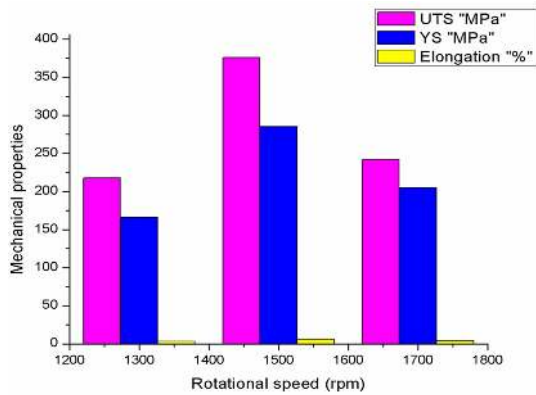


Figure 8: Effect of rotational speed on tensile strength

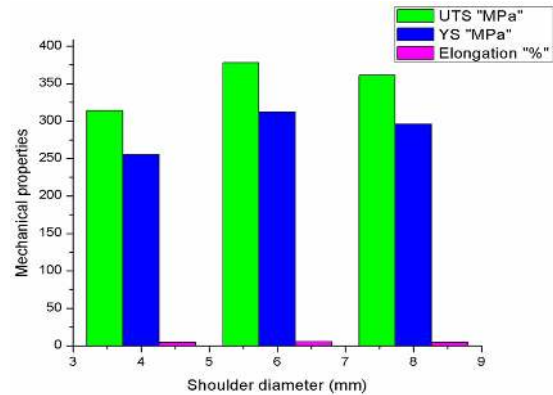


Figure 10: Effect of shoulder diameter on tensile strength

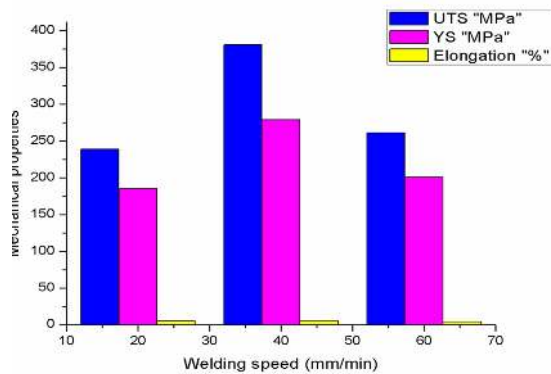


Figure 9: Effect of welding speed on tensile strength

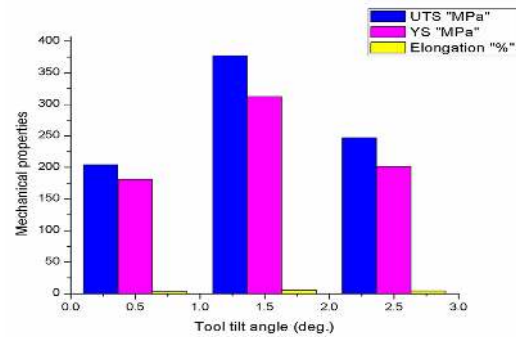


Figure 11: Effect of tool tilt angle on tensile strength

material flow in the SZ, weld region was classified into

three states such as insufficient material flow, balance material flow and excessive material flow state [24, 25]. The balance material flow state can be obtained by choosing a

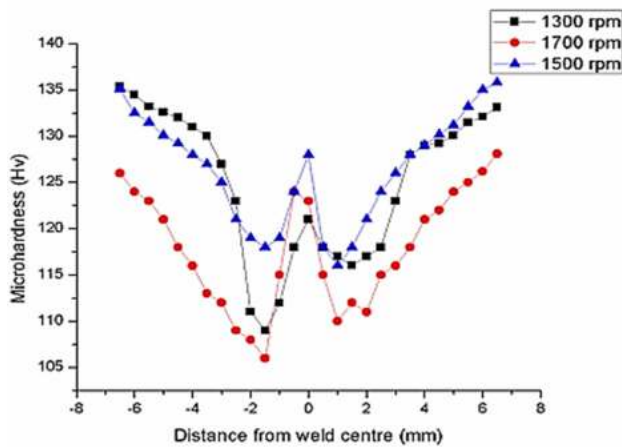


Figure 12: Effect of rotational speed on microhardness

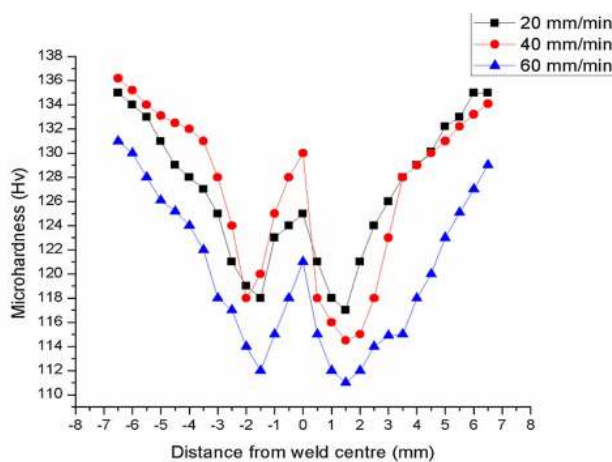


Figure 13: Effect of welding speed on microhardness

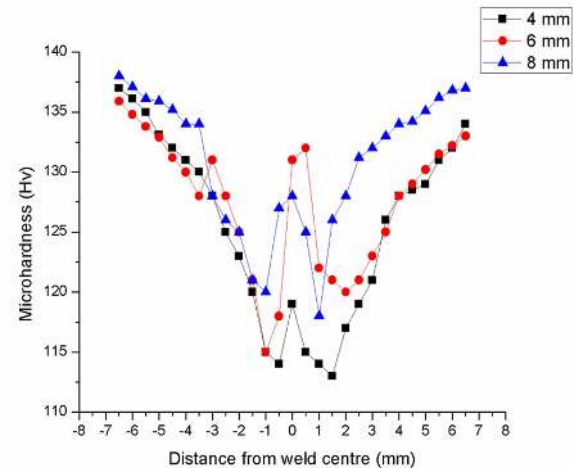


Figure 14: Effect of shoulder diameter on microhardness

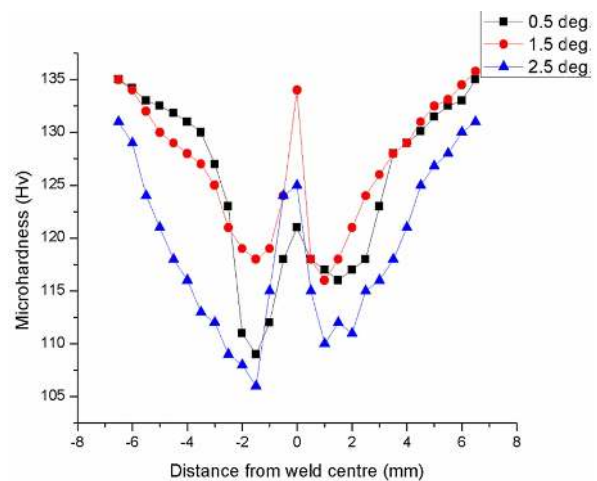


Figure 15: Effect of tilt angle on microhardness


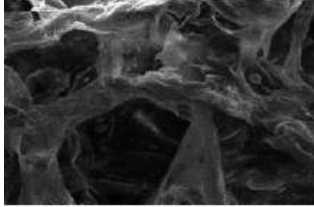

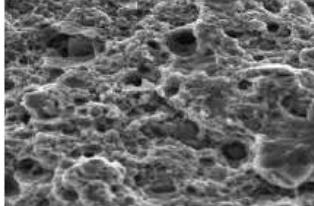

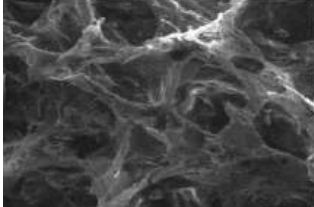
proper combination of process parameters. The excessive and insufficient material flows will easily produce defects. It is attributed due to heat input [24].

4.1 Relationship between tool rotational speed and joint quality

The tool rotational speed is the most predominant process parameter in FSW. Because, the rotational speed has a direct relationship to the supplied heat energy [22]. Hence, the quality of the FSW joints are dependent on heat supplied and heat dissipation during FSW. From the Table 5, it is understood that the joint fabricated from the rotational speed of 1500 rpm (constant 40 mm/min, 6 mm and 1.5) exhibited higher tensile strength (381 MPa) due to the defect free and sound joint. Also, balanced material flow could be achieved. Moreover, the joint had a uniform distribution of fine Al_2Cu precipitate in α -aluminum matrix and

fine recrystallized grains ($7.09 \mu\text{m}$). Further, increasing rotational speed to 1900 rpm, the tensile properties were considerably reduced; it may be attributed to high heat input, which in turn leads to precipitation of precipitates, grain coarsening and void defect [26]. The average SZ hardness of the joint fabricated from the rotational speed of 1500 rpm yielded 128 HV than their counter joints due to formation of fine and recrystallized grains. From the fracture surface morphology, it is inferred that that joint (1500 rpm) had fine and deep dimples, which could indicate that the large stretch zone was present at the tip of the crack and the fracture was ductile mode.

Table 5: Effect of tool rotational speed on macrograph and fracture pattern

Tool rotational speed "rpm"	Macrograph	Fractograph	Observation
1300			GS: 10 μm Fracture location: SZ Fracture Pattern: Large elongated dimples
1500			GS: 7 μm Fracture location: SZ/TMAZ Fracture Pattern: Fine dimples
1700			GS: 12 μm Fracture location: SZ/TMAZ Fracture Pattern: Coarse and elongated dimples

GS - Grain size

4.2 Relationship between welding speed and joint quality


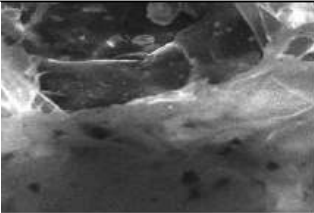

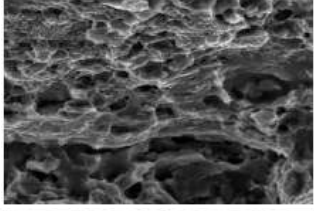

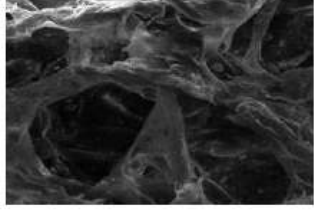
The rate of heat generation of thermal cycle during FSW is a strong function of welding speed [27]. During FSW, most of the fine eutectic element of Cu in AA2014-T6 aluminum alloy are dissolved and uniformly distributed in the α -aluminum matrix. The rate of heat dissipation in the thermal cycle retains this solute in the aluminum matrix. Of the five joints, the joint fabricated using a welding speed of 40 mm/min yielded higher tensile strength than their counterpart. Due to the formation of defect free and sound joints. Moreover, the formation of fine eutectic Cu element uniformly distributed over the alpha aluminum matrix. At low welding speed (10 mm/min), the joint consists of coarse Cu particle which in-turn reduces the tensile strength. Similarly, the joint fabricated from higher welding speed of 70 mm/min consists of channel like defect in the retreating side of the SZ, due to insufficient material flow state and consist of coarse grains. The reason for higher tensile strength was achieved by the joint fabricated using a welding speed of 40 mm/min (under constant rotational speed of 1500 rpm, shoulder diameter of 6 mm and tilt angle of 1.5), the optimum heat input creates balanced material

flow state and density distribution of precipitates (Al_2Cu) in the SZ.

4.3 Relationship between shoulder diameter and joint quality

The shoulder diameter is another important process parameters in the FSW. It has a direct relationship to the heat input due to friction in FSW cycle [28–31]. The material transfer occurs due to rotation of tool shoulder. In the FSW, one third of material moves under the influences of shoulder diameter rather than the pin. The tool pins generate heat and stir the materials in the SZ and provides additional friction treatment and prevents the plasticized material escaping from the weld region. From the heating aspects to maintain the proper tool shoulder diameter and pin to achieve maximum strength and homogeneity of microstructure in FSW joints. Figure 3c shows the effect of tool shoulder diameter on tensile strength of FSW joints. It can be seen that the tensile strength of friction stir welded joints, increased with increasing the tool shoulder diameter for a fixed tool rotational speed of 1500 rpm, welding speed of 40 mm/min and tool tilt angle of 1.5°. From the

Table 6: Effect of welding speed on macrograph and fracture pattern

Welding speed “rpm”	Macrograph	Fractograph	Observation
20			GS: 12 μm Fracture location: SZ/TMAZ Fracture Pattern: Coarse elongated dimples
40			GS: 8 μm Fracture location: SZ/TMAZ Fracture Pattern: Fine dimples
60			GS: 11 μm Fracture location: SZ Fracture Pattern: Elongated dimples

GS - Grain size

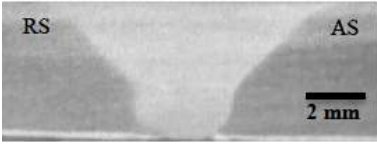
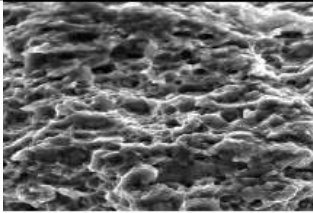

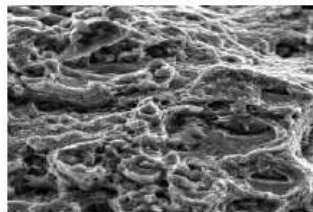
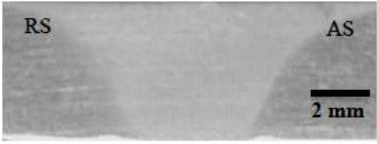
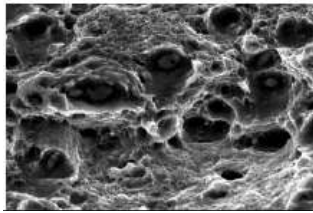
observation the following inferences can be obtained. The bigger shoulder diameter (>8 mm) leads to wider contact area and resulted in wider TMAZ region and HAZ region and subsequently reduces the strength. The smaller shoulder diameter (<4 mm) produced insufficient material flow state, which in turn lack of filling and poor material consolidation due to low contact area. Also, the vertical flow of material was lower. Of the five joints fabricated using tool shoulder diameters, the joint fabricated from the 6 mm shoulder diameter yielded superior tensile strength (378 MPa) than their counter joints. A bigger shoulder diameter may lead to wider TMAZ and heat affected zone rather than the smaller diameter, due to high peak temperature developed in the SZ (>10 mm) during FSW. It produced grain coarsening, warm hole, dissolution of precipitates and coarsening of some of few precipitates [23]. Moreover, excessive material flow causes thinning effect and reduces the effective sheet thickness and results in inferior tensile strength in FSW joints of AA2014 aluminum alloy. The area below the shoulder was smaller and produced less heat input that causes insufficient material flow and poor material consolidation. Hence, the joints yielded lower strength. The joint fabricated from tool shoulder diameter of 6 mm produced higher tensile strength than other joints. The reason for higher strength and hardness may attribute: suf-

ficient heat input causes uniform distribution of precipitates and finer recrystallized grains during FSW.

4.4 Relationship between tool tilt angle and joint quality

The tool tilt angle is defined as the angle at which the FSW tool is positioned relative to the work piece surface, *i.e.* 0° tilted tool is positioned perpendicular to the work piece surface. It affects the heat generation rate and compressive force [32, 33] which subsequently affect the material flow; tensile strength [34]. Figure 2 shows the macrostructure of different tilt angles. Minor defects (voids and cracks) were observed for tilt angles 0° and 3.0°, whereas defect free macrostructures were noticed for tilt angles 0.5°, 1.5°, and 2.5°. Additionally, the shape of the stir zone also varied with variation in tool tilt angles. The incomplete or lack of fill defect was observed on the surface of weld made at 0° tool tilt angle, due to insufficient material flow around the pin. Additionally, the tool tilt angle increases from 0.5° to 2.5° with an increment of 1°, the increase in tool tilt angle resulted increase in heat generation and high forging force [35, 36]. When the pin is threaded it can also accelerate more volume of plasticized material and pushes the

Table 7: Effect of shoulder diameter on macrograph and fracture pattern

Tool shoulder diameter "mm"	Macrograph	Fractographs	Observation
4			GS:10 μm Fracture location: SZ Fracture Pattern: Fine dimples
6			GS:7 μm Fracture location: SZ/TMAZ Fracture Pattern: fine and deep dimples
8			GS:9 μm Fracture location: SZ/TMAZ Fracture Pattern: shallow dimples


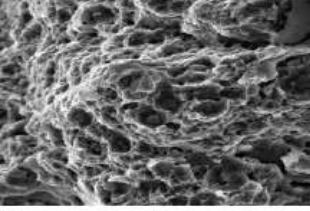

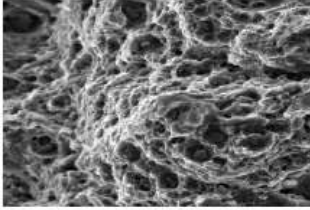

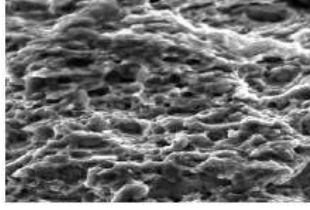
GS - Grain size

material in a downward direction [37]. However, the weld made at 3.5° tool tilt angle causes thinning effect on the localized weld region. Hence, effective sheet thickness was reduced which resulted in poor weld strength, because the gap between the tool and the work piece made from the tilt of the tool expands with increasing the tilt angle. Thus, by increasing the tilt angle, the plasticized material escapes easily from the underside of the tool shoulder [38, 39]. Consequently, a discontinuity occurs in the weld, which leads to the formation of some voids at the surface. Therefore, there is an optimum tool tilt angle in FSW; which was found to be 1.5° for AA2014-T6 aluminum alloy. Another one important criteria in the FSW process in aluminum alloy weld is onion ring formation. The significance of the onion ring formation is material flow around the pin, in which it indicates the flow of plasticized material in the stir zone of uniform pattern [40]. At the weld made with 0.5° tool tilt angle generated a number of concentric onion rings (Figure 19d). Even though, two no of onion ring region was formed over to another when welded with 1.5° tool tilt angle (Figure 19e), likewise, when the FSW made using 2.5° tilt angle produced three number of onion ring region one over by another one (Figure 19f). It could be in-

dicative that the flow of material in downward and upward in the stir zone

From the Table 4, the maximum tensile strength of 377 MPa is exhibited, when welded with 1.5° tool tilt angle. The other joints have lower tensile strength due to the redistributed Alclad which penetrates into the SZ, which may be a preferred crack propagation path to tensile testing, because it is much softer than aluminum alloy. Therefore, the morphology of the redistributed Alclad in the SZ has significant influences on the tensile properties of the FSW joint, as shown in Figure 8f. The higher tool tilt angle makes the redistributed Alclad in the SZ more dispersed, and this prevents the redistributed Alclad from being a preferred crack propagation path to the tensile test. The 90% of fracture location in FSW always at the interface between TMAZ and SZ on advancing side; this is due to thermal softening and grain coarsening during thermal cycle [23, 24]. In the weld made with 0.5° tilt angle the fracture occur to the SZ due to insufficient consolidation, because the lower tilt angle produces less heat generation and lower forging force, this is the reason for the fracture occurred in the stir zone. The fracture location of FSW made with 2.5° tool tilt angle was on the AS, because, the effective sheet thickness was considerably reduced. The average microhardness of the stir

Table 8: Effect of tool tilt angle on macrograph and fracture pattern

Tool tilt angle "deg."	Macrograph	Fractographs	Observation
0.5°			GS:14 μm Fracture location: SZ Fracture Pattern: Elongated dimples
1.5°			GS:7.89 μm Fracture location: SZ/TMAZ Fracture Pattern: Fine and deep dimples
2.5°			GS:12 μm Fracture location: SZ/TMAZ Fracture Pattern: fine dimples with shear ridges.

GS - Grain size

zone of 134 HV was achieved, when the weld made to the tilt angle of 1.5°.

4.5 Influence of FSW parameters on failure pattern

From the Tables 5-8, it is understood that the FSW parameters had a significant effect on the fracture pattern of the friction stir welded joints. The base material has undergone transgranular ductile fracture surfaces covered with fine dimples of varying size and shape, some deep voids and enlarged dimples were also observed on the fractured surface. The fractured surface of the welds invariably showed dimples of varying size and shape separated from tear edges. Which an indication of ductile failure [41] except some low heat input joints produced low rotational speed (1300 rpm), high welding speed (60 mm/min), small shoulder diameter (4 mm) and low tilt angle (0.5°). The fracture propagates from the breakages of secondary precipitates rich in Cu and Mn, which initiate the formation of micro voids at the grain boundary. Failure pattern was brittle in low heat input joints and fracture surface covered with layered ridges. At the high heat input showed ductile fracture mode with large and elongated dimples.

4.6 TEM micrograph

Figure 20 show the TEM micrograph of precipitates distribution across the different region of the joint fabricated with the rotational speed of 1500 rpm, welding speed of 40 mm/min, shoulder diameter of 6 mm and tilt angle of 1.5°. Figure 20a, 20b, 20c show the precipitates distribution in the TMAZ-retreating side, SZ and TMAZ-advancing side respectively. Based on the TEM with EDS analysis the base material consists of Al₂Cu and Fe-Mn-Al intermetallic. The average size of the particle was 60 nm. The reason for the joint exhibiting higher strength and hardness were, an optimum heat input in the SZ would lead to higher level of precipitate dissolution of the strengthening precipitates and a large amount of solute will be retained in the aluminum matrix of the weld region, than that observed in the welds with low heat input. This may be influenced by variation in the retained dislocation density with in the SZ, peak temperature may be expected to be higher for the high level for high deformation and it can inhibit Guiner Preston Zone (GP-zone) formation [30]. Hence, the high hardness of optimized welding process parameter may be attributed to the solid solution strengthening combined with the formation of sub grains. Also, the SZ hardness was improved by the formation of (Cu Fe Mn) Al₆ precipitates.

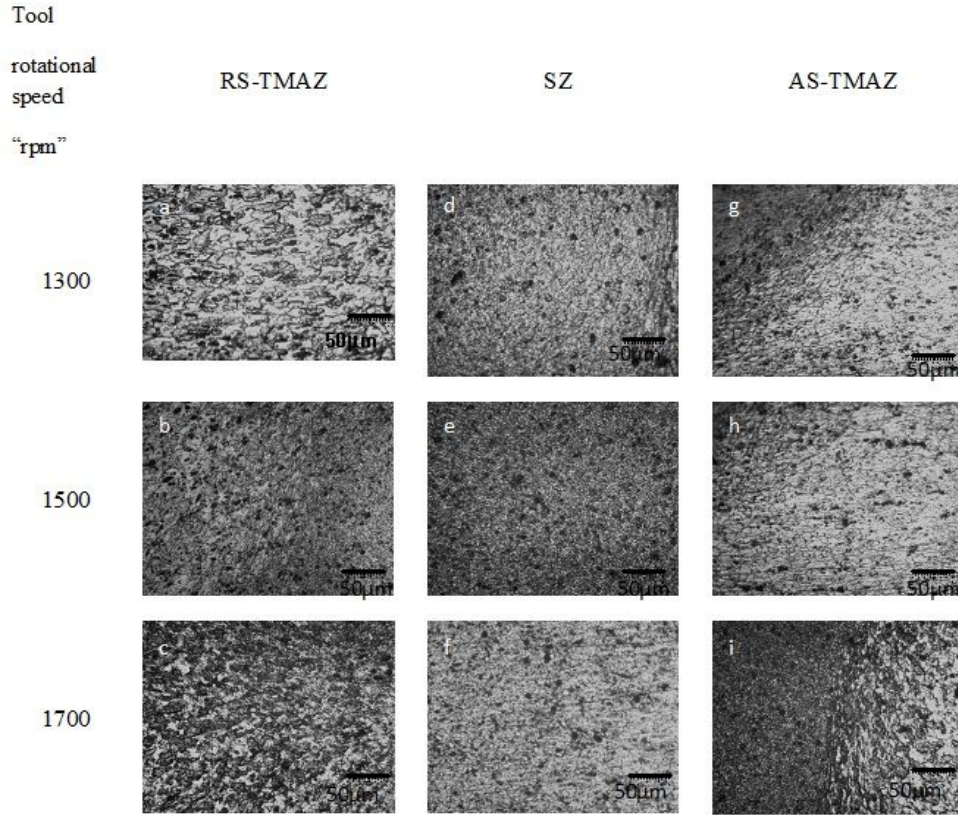


Figure 16: Effect of tool rotational speed on micrograph

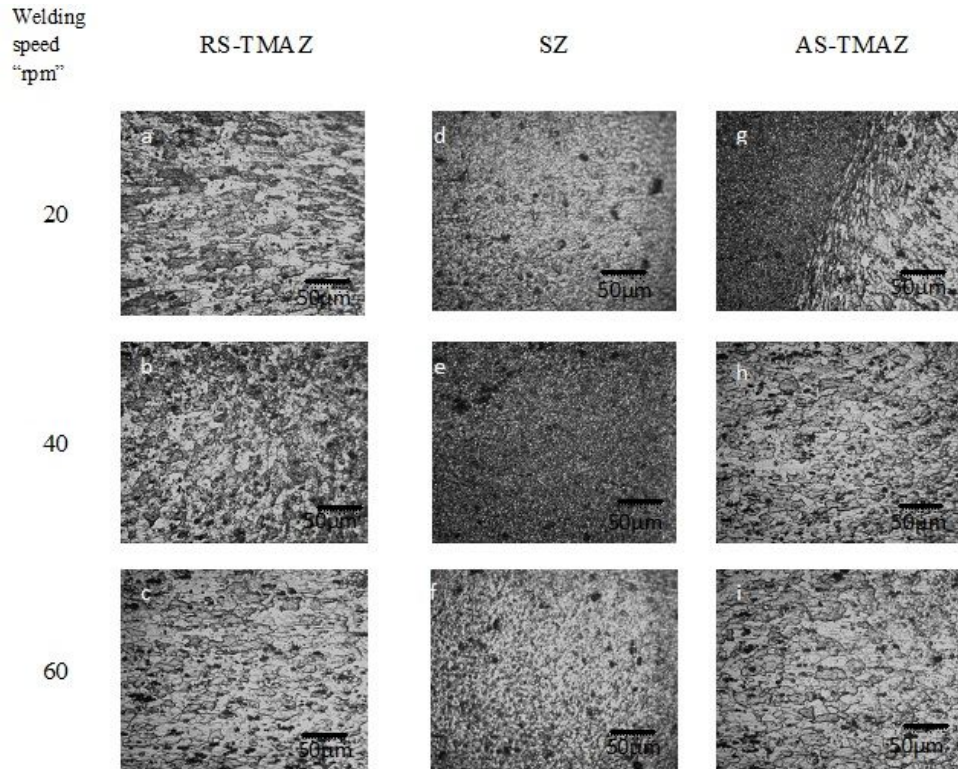


Figure 17: Effect of welding speed on micrograph

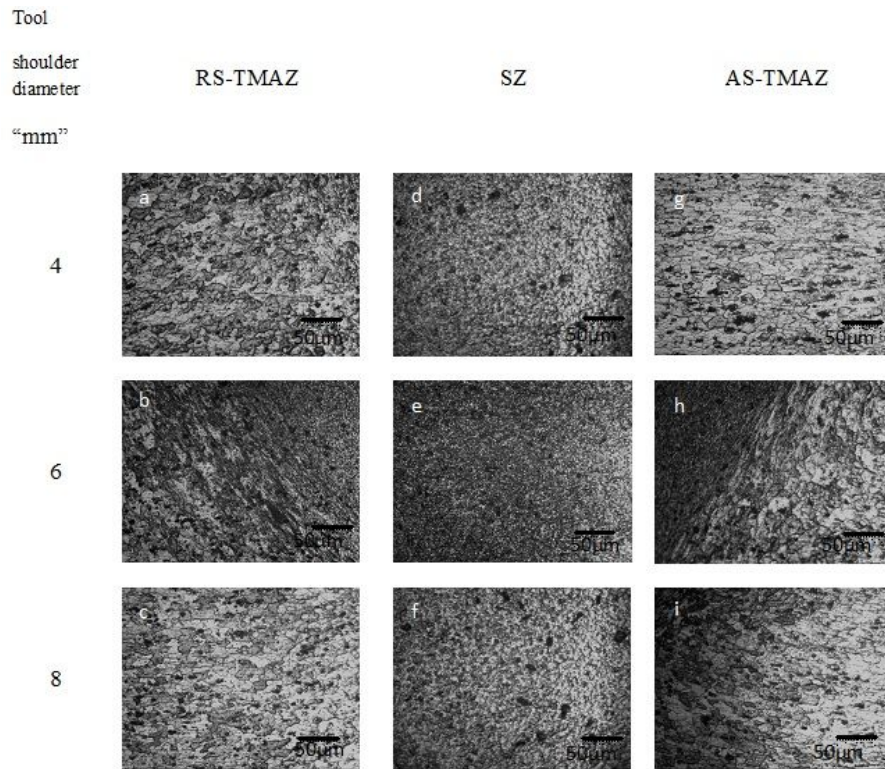


Figure 18: Effect of shoulder diameter on micrograph

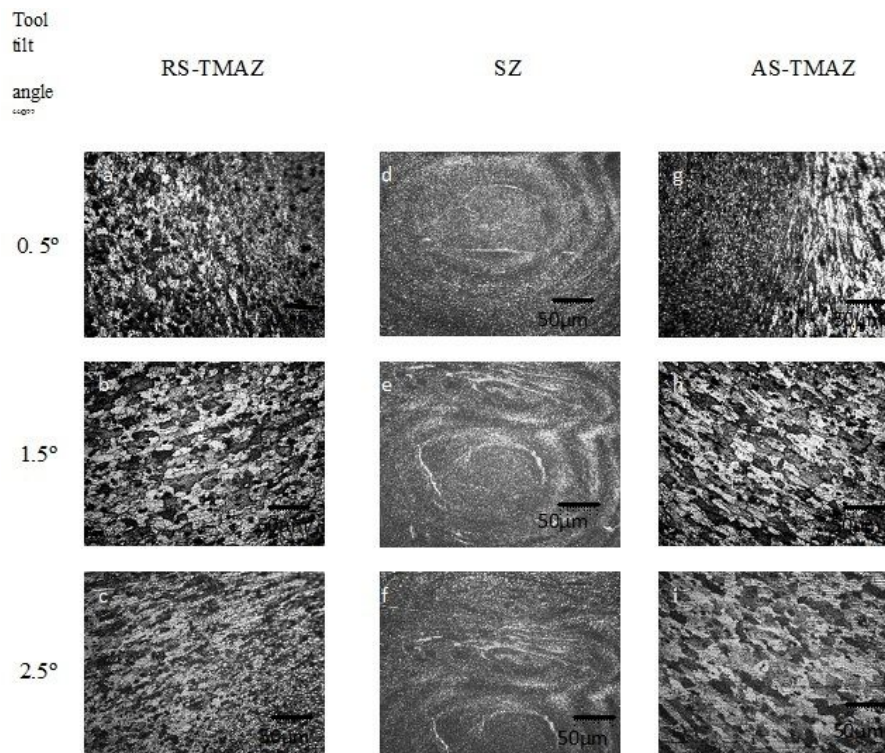


Figure 19: Effect of tool tilt angle on micrograph

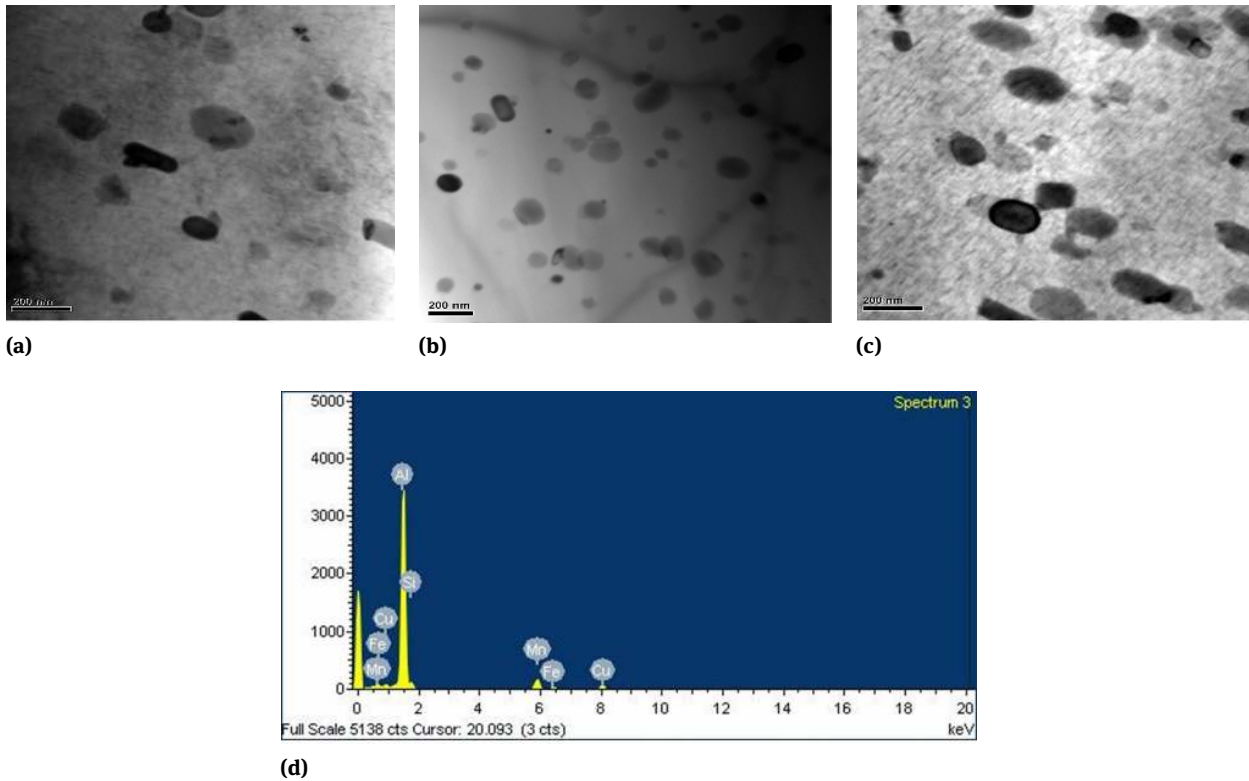


Figure 20: TEM micrograph of a) TMAZ on RS, b) SZ, c) TMAZ on AS, d) EDS result of SZ

5 Conclusion

The following inferences can be obtained from this investigation.

1. Microstructural characteristics and mechanical properties could be effectively controlled by varying any one process parameter and by keeping others constant.
2. The sound welded joint was obtained at the tool rotational speed of 1500 rpm, welding speed of 40 mm/min, shoulder diameter of 6 mm and tilt angle of 1.5° . It could be due to the balanced material flow around the pin with optimum FSW parameters.
3. The increase in solute concentration has produced a number of sub grains in the SZ due to optimal heat input, which lead to increased tensile properties owing to a reduction in the density distribution of coarse second phase particle (Al_2Cu).
4. The hardness distribution is in good agreement with the obtained microstructure and shows two soft regions on both the sides of each joint.
5. Tensile properties of the joint are lower than those of base material; the maximum efficiency in terms

of UTS and % elongation are 83% and 5.8% respectively.

6. Most of the FSW joints were fractured at the interface between SZ/TMAZ in advancing side, due to the different velocity gradient of plasticized material between advancing side and retreating side, which in turn produced different microstructures.

Acknowledgement: The authors are thankful to Aeronautical Development Agency (ADA), Bangalore for providing financial support through Project No: FSED: 83.07.03 to carry out this research work under project entitled “Development of friction stir welding technology for aircraft structure”.

References

- [1] Dietrich D., Nickel D., Krause M., Formation of intermetallic phases in diffusion welded joints of aluminium and magnesium alloys, *J. Mater. Sci.*, 2011, 46, 357-364.
- [2] Mishra R.S., Ma Z.Y., Frictions stir welding and processing, *Mater. Sci. Eng.*, 2005, 50, 1-78.
- [3] Nandan R., DebRoy T., Bhadeshia H.K.D.H., Recent advances in friction-stir welding-process, Weldment structure and properties,

- Prog. Mater. Sci., 2008, 53, 980-1023.
- [4] Scialpi A., De Filippis L.A.C., Cavaliere P., Influence of shoulder geometry on microstructure and mechanical properties of friction stir welded 6082 aluminum alloy, *Mater. Des.*, 2007, 28, 1124-1129.
 - [5] Xu W.F., Liu J.H., Luan G.H., Dong C.L., Temperature evolution, microstructure and mechanical properties of friction stir welded thick 2219-O aluminum alloy joints, *Mater. Des.*, 2009, 30, 1886-1893.
 - [6] Genevois C., Deschamps A., Denquin A., Doisneau-Cootignies B., Quantitative investigation of Precipitation and mechanical behavior for AA2024 friction stir welds, *Acta Mater.*, 2005, 53, 2447-2458.
 - [7] Upadhyay P., Reynolds A.P., Effects of thermal boundary conditions in friction stir welded AA7050-T7 sheets, *Mater. Sci. Eng. A*, 2010, 527, 1537-1543.
 - [8] Fu R.D., Sun Z.Q., Sun R.C., Li Y., Liu H.J., Lei L., Improvement of weld temperature distribution and mechanical properties of 7050 aluminum alloy butt joints by submerged friction stir welding, *Mater. Des.*, 2011, 32, 4825-4831.
 - [9] Mofid M.A., Abdollah-Zadeh A., Malek Ghaini F., The effects of water cooling during dissimilar friction stir welding of Al alloy to Mg alloy, *Mater. Des.*, 2012, 36, 161-167.
 - [10] Zettler R., Dissimilar Al to Mg alloy friction stir welds, *Adv. Eng. Mater.*, 2006, 8, 415-421.
 - [11] McLean A.A., Powell G.L.F., Brown I.H., Linton V.M., Friction stir welding of magnesium alloy AZ31B to aluminum alloy 5083, *Sci. Technol. Weld. Join.*, 2003, 8, 462-464.
 - [12] Zhang F., Su X., Chen Z., Nie Z., Effect of welding parameters on microstructure and mechanical properties of friction stir welded joints of a super high strength Al-Zn-Mg-Cu aluminum alloy, *Mater. Des.*, 2015, 67, 483-491.
 - [13] Muthu M.F.X., Jayabalan V., Effect of pin profile and process parameters on microstructure and mechanical properties of friction stir welded Al-Cu joints, *Trans. Non-ferr. Met. Soc. China*, 2016, 26, 984-993.
 - [14] Mao Y., Ke L., Liu F., Huang Ch., Chen Y., Liu Q., Effect of welding parameters on microstructure and mechanical properties of friction stir welded joints of 2060 aluminum lithium alloy, *Int. J. Adv. Manuf. Technol.*, 2015, 81, 1419-1431.
 - [15] Xu W., Liu J., Zhu H.Q., Fu L., Influence of welding parameters and tool pin profile on microstructure and mechanical properties along the thickness in a friction stir welded aluminum alloy, *Mater. Des.*, 2013, 47, 599-606.
 - [16] Ramachandran K.K., Murugan N., Shashi Kumar S., Influence of tool traverse speed on the characteristics of dissimilar friction stir welded aluminum alloy, AA5052 and HSLA steel joints, *Arch. Civil Mech. Eng.*, 2015, 15, 822-830.
 - [17] Sharma C., Dwivedi D.K., Kumar P., Effect of welding parameters on microstructure and mechanical properties of friction stir welded joints of AA7039 aluminum alloy, *Mater. Des.*, 2012, 36, 379-390.
 - [18] Singh G., Singh K., Singh J., Effect of Process Parameters on Microstructure and Mechanical Properties in Friction Stir Welding of Aluminum Alloy, *Trans. Indian. Inst. Met.*, 2011, 64, 325-330.
 - [19] Cai B., Zheng Z.Q., He D.Q., Li S.C., Li H.P., Friction stir weld of 2060 Al-Cu-Li alloy: Microstructure and mechanical properties, *J. All. Compd.*, 2015, 649, 19-27.
 - [20] Dong P., Li H., Sun D., Gong W., Liu J., Effects of welding speed on the microstructure and hardness in friction stir welding joints of 6005A-T6 aluminum alloy, *Mater. Des.*, 2013, 45, 524-531.
 - [21] Liu X., Lan S., Ni J., Analysis of process parameters effects on friction stir welding of dissimilar aluminum alloy to advanced high strength steel, *Mater. Des.*, 2014, 59, 50-62.
 - [22] Heurtier P., Desrayaud C., Montheillet F., A thermomechanical analysis of the friction stir welding process, *Mater. Sci. Forum*, 2002, 1537, 396-402.
 - [23] Rajendran C., Srinivasan K., Balasubramanian V., Balaji H., Selvaraj P., Identifying combination of friction stir welding parameters to maximize strength of lap joints of AA2014-T6 aluminium alloy, *Austral. J. Mech. Eng.*, 2017, 17(2), 1304843.
 - [24] Liu H.J., Zhang H.J., Yu L., Effect of welding speed on microstructures and mechanical properties of underwater friction stir welded 2219 aluminum alloy, *Mater. Des.*, 2011, 32, 1548.
 - [25] Kumar K., Kailas S.V., The role of friction stir welding tool on material flow and weld formation, *Mater. Sci. Eng. A*, 2008, 485, 367.
 - [26] Lomolino S., Tovo R., Dos Santos J., On the fatigue behavior and the design curve of friction stir butt welded Al alloy, *Int. J. Fatigue*, 2005, 27, 305-316.
 - [27] Ma Z.Y., Sharma S.R., Mishra R.S., *Scripta Mater.*, 2006, 54, 1623.
 - [28] Lima E.B.F., Wegener J., Dalle D., Goerigk G., Wroblewski T., Buslaps T., Dependence of the microstructure, residual stresses and texture of AA6013 friction stir welds on the welding processes, *Z Metallk.*, 2003, 94(8), 908-915.
 - [29] Oosterkamp A., Djapic Oosterkamp L., Nordeide A., Kissing bond phenomena in solid state welds of aluminum alloys, *Weld J.*, 2004, 83, 225-231.
 - [30] Chen Y., Liu H., Feng J., Friction stir welding characteristics of different heat-treated-state 2219 aluminum alloy plates, *Mater. Sci. Eng. A*, 2006, 420, 21-25.
 - [31] Elangovan K., Balasubramanian V., Influences of tool pin profile and tool shoulder diameter on the formation of friction stir processing zone in AA6061 aluminum alloy, *Mater. Des.*, 2008, 293, 362-373.
 - [32] Nandan R., Debroy T., Badheshia H.K.D.H., Recent advances in friction-stir welding - Process, weldment structure and properties, *Prog. Mater. Sci.*, 2008, 53, 980-1023
 - [33] Muhayat N., Zubaydi A., Sulistijono, Yuliadi M.Z., Effect of tool tilt angle and tool plunge depth on mechanical properties of friction stir welded AA 5083 joints, *Appl. Mech. Mater.*, 2014, 493, 709-714.
 - [34] Kimapong K., Watanabe T., Effect of welding process parameters on mechanical property of FSW lap joint between aluminum alloy and steel, *Mater. Trans.*, 2005, 46, 2211-2217.
 - [35] Pande S.V., Badheshia V.J., Effect of tool pin offset on mechanical and metallurgical properties of dissimilar FSW joints of AA6061 T6 aluminum alloy and copper material, In: *Proc. Int. Weld. Congr. (IC2014)*, New Delhi, India, 2014, 697-703.
 - [36] Galvo I., Leal R.M., Loureiro A., Rodrigues D.M., Material flow in heterogeneous friction stir Welding of aluminum and copper thin sheets, *Sci. Technol. Weld. Join.*, 2010, 15, 654-660.
 - [37] Rajendran C., Srinivasan K., Balasubramanian V., Balaji H., Selvaraj P., Identifying the combination of friction stir welding parameters to attain maximum strength of AA2014-T6 aluminum alloy joints, *Adv. Mater. Proc. Tech.*, 2018, 4(1), 100-119.
 - [38] Rajendran C., Srinivasan K., Balasubramanian V., Balaji H., Selvaraj P., Effect of tool tilt angle on strength and microstructural characteristics of friction stir welded lap joints of AA2014-T6 aluminum alloy, *Trans. Non-ferrous Met. Soc. China*, 2019, 29,

1824-1835.

- [39] Seghalani A.R., Givi M.K.B., Nasiri A.M., Bahemmat P., Investigation on the effect of tool material, geometry and tilt angle on friction stir welding of pure titanium, *J. Mater. Manuf.*, 2010, 19, 955-962.
- [40] Krishnan K.N., On the formation of onion rings in friction stir welds, *Mater. Sci. Eng. A*, 2002, 327, 246-251.
- [41] Xu W., Liu J., Luan G., Dong C., Temperature evaluation, microstructure and mechanical properties of friction stir welded thick 2219-O aluminum alloy joints, *Mater. Des.*, 2009, 1886-1893.